fishes

MDPI

Article

Evaluation of Hypoxia Tolerance and Cloning-Expression Analysis of Related Genes in Hybrid Fish Derived from *Megalobrama amblycephala* × *Xenocypris davidi* Bleeker

Zhong Tang [1,2,†], Xinxin Yu [1,2,†], Xin Chen [1,2], Junwen Liang [1,2], Yangyang Tu [1,2], Zhifeng Zhou [1,2], Faxian Yu [1,2], Chun Zhang [1,2], Siyu Fan [1,2,*] and Min Tao [1,2,*]

[1] Engineering Research Center of Polyploid Fish Reproduction and Breeding of the State Education Ministry, College of Life Sciences, Hunan Normal University, Changsha 410081, China; tz18570752186@163.com (Z.T.); yxx1758155428@163.com (X.Y.); 15387515292@163.com (X.C.); 19873671956@163.com (J.L.); 18873061376@163.com (Y.T.); zhuisuizhumeng@126.com (Z.Z.); yfxfafafa101@163.com (F.Y.); zhangchun421@163.com (C.Z.)
[2] Yuelushan Laboratory, Changsha 410128, China
* Correspondence: minmindiu@126.com (M.T.); fsy@hunnu.edu.cn (S.F.)
† These authors contributed equally to this work.

Abstract

The diploid distant hybrid (2nBY) derived from female blunt snout bream (*Megalobrama amblycephal*, BSB) × male Bleeker's yellow tail (*Xenocypris davidi* Bleeker, YT). To investigate the hypoxia tolerance and the regulatory mechanisms of hypoxia-inducible factor-1α/2α (*hif-1α/2α*) in 2nBY, BSB, and YT, experiments consisting of 24 h of hypoxia treatment (DO = 2.0 ± 0.1 mg/L) followed by 6 h of reoxygenation were conducted. The loss of equilibrium critical oxygen pressure (*LOEcrit*), gill tissue structure, and antioxidant indices, as well as the full-length sequences and expression of *hif-1α/2α* in 2nBY, BSB, and YT, were compared. The results showed that the *LOEcrit* value of 2nBY was significantly lower than that of BSB but higher than that of YT ($p < 0.05$). After hypoxia treatment, the changes in gill tissue structure and antioxidant indices of 2nBY were less obvious than those of BSB, and the recovery rate was faster after reoxygenation. Sequence analysis revealed high similarity of *hif-1α/2α* between YT and 2nBY. After hypoxia treatment, *hif-1α/2α* were upregulated in the liver but showed distinct gill expression among the three groups. Their gill expression differences may contribute to varied hypoxic tolerance. Distant hybridization between BSB and YT successfully generated hybrid offspring with enhanced hypoxia tolerance relative to BSB. These results provide theoretical and technical support for the breeding of a new hypoxia-tolerant germplasm resource of bream.

Keywords: hypoxia tolerance; distant hybridization; *hif-1α*; *hif-2α*

Key Contribution: 2nBY has better hypoxia tolerance than BSB, and this advantage may be derived from YT. This study provided theoretical and technical support for the breeding of new hypoxia-tolerant bream germplasm.

Check for updates

Academic Editor: Zhishuai Hou

Received: 6 March 2026
Revised: 6 April 2026
Accepted: 13 April 2026
Published: 15 April 2026

Copyright: © 2026 by the authors. Licensee MDPI, Basel, Switzerland. This article is an open access article distributed under the terms and conditions of the Creative Commons Attribution (CC BY) license.

1. Introduction

Dissolved oxygen (DO) is a key environmental parameter in water bodies and is crucial for fish survival [1]. When dissolved oxygen in water decreases, it affects the growth and development of fish, and can even lead to death in severe cases [2]. However, fish species vary in hypoxia tolerance: crucian carp (*Carassius carassius*) is capable of

surviving in hypoxic environments [3], while silver carp (*Hypophthalmichthys molitrix*) is not [4]. Additionally, the hypoxia tolerance of fish is also influenced by their body size, age, environmental adaptability, and physiological state, and these factors collectively determine their survival ability in hypoxic conditions [5].

Distant hybridization, as a vital technique in aquatic breeding, can break interspecific reproductive isolation and create new germplasm with heterosis [6]. Blunt snout bream (*Megalobrama amblycephala*, BSB, 2n = 48) is favored by the market for its fast growth and tender meat, but it has weak hypoxia tolerance. During cultivation, it often dies in large numbers due to rapid drops in dissolved oxygen in water, causing serious economic losses [7]. In contrast, Bleeker's yellow tail (*Xenocypris davidi* Bleeker, YT, 2n = 48) exhibits excellent hypoxia tolerance, capable of surviving in hypoxic sludge environments and purifying water quality [8]. Previously, our research team carried out inter subfamily distant hybridization using BSB as the female parent and YT as the male parent, successfully obtaining diploid hybrid fish (2nBY) [9]. It has been confirmed that 2nBY exhibits significant advantages in growth rate and meat quality [10]. However, the differences in hypoxia tolerance between 2nBY and its parents, as well as the related molecular regulatory mechanisms, remain unclear.

The ability of fish to cope with hypoxic environments can be comprehensively evaluated through hypoxia-related indicators such as behavior, physiology, and biochemistry [11]. Behaviorally, critical oxygen pressure for loss of equilibrium (*LOEcrit*) is a key indicator of hypoxia tolerance, with lower values indicating stronger tolerance [12]. At the histological level, fish gills perform a variety of important physiological functions, such as gas exchange, ion regulation, and food filtration [13]. Under hypoxic conditions, significant changes occur in the morphology and structure of fish gills. When the oxygen concentration returns to normal levels, their morphology and structure can recover to a certain extent, a phenomenon known as "gill remodeling" [14]. The remodeling capacity of fish gills directly determines the gas exchange efficiency and recovery ability of fish in hypoxic environments. Physiologically and biochemically, hypoxia induces oxidative stress and reactive oxygen species (ROS) accumulation [15]. Superoxide dismutase (SOD), as a core antioxidant enzyme, can reduce oxidative damage by scavenging ROS [16]. Catalase (CAT), in turn, catalyzes the decomposition of hydrogen peroxide into oxygen and water, thereby further scavenging ROS and reducing damage to cells [17]. Malondialdehyde (MDA), as the end product of lipid peroxidation, directly reflects the degree of oxidative damage to the organism [18].

Hypoxia-inducible factors (Hifs) are heterodimeric transcription factors that consist of a group of structurally homologous α-subunits and a common β-subunit, and they play a key role in helping animals maintain the homeostasis and balance of oxygen concentration in the body [19]. Hif-αs are extremely sensitive to changes in oxygen concentration and are the main functional subunits in hypoxic regulation, so the activity of hypoxia-inducible factors mainly depends on the activity of Hif-αs [20]. To date, four major types of Hif-αs have been identified, namely Hif-1α, Hif-2α, Hif-3α, and Hif-4α [21,22]. Hif-1α and Hif-2α can bind to the hypoxia response elements in the promoter region of target genes. This binding regulates a series of downstream pathways, including glucose metabolism, lipoprotein metabolism, angiogenesis, and antioxidant processes [23,24]. These factors play a core role in the hypoxic adaptation of fish. Cloning the full-length sequence of key genes, analyzing protein structure, and deciphering their expression patterns are core steps to explore the molecular mechanism of fish hypoxia tolerance.

This study systematically compares the differences in hypoxia-related indicators and the expression of *hif-1α* and *hif-2α* genes between 2nBY and its parents through hypoxia

and reoxygenation treatments, providing theoretical support and technical references for the breeding of a new hypoxia-tolerant germplasm resource of bream.

2. Materials and Methods

2.1. Experimental Fish

The experimental fish with a body mass of 10.0 ± 0.5 g and a body length of 9.0 ± 0.5 cm were obtained from Hunan Fish Genetics and Breeding Center (Wangcheng, Hunan, China). The fish were randomly divided and reared temporarily in aquaria (40 × 60 × 50 cm, L:W:H) for one week, with 30 individuals per container. Environmental parameters were as follows: dissolved oxygen (DO) concentration of 7.5 ± 0.5 mg/L, water temperature maintained at 25.0 ± 0.1 °C, and pH value kept at 7.5 ± 0.1. During the temporary feeding period, the feed brand used was Tongwei Extruded Compound Feed for Fish (CH402) (Chengdu, China). Feeding was stopped 48 h before the experiment, and individuals with healthy body condition and normal activity were selected for the experiment when the mortality rate was observed to be below 5%.

2.2. Determination of LOEcrit

The total number of experimental fish used for determining *LOEcrit* was 30 for BSB, YT and 2nBY, respectively. Ten individuals each of 2nBY and its parents were acclimated in aquaria (40 × 60 × 50 cm, L:W:H) for 24 h prior to the sealed experiment, with the experiment repeated three times. Dissolved oxygen was gradually and steadily reduced in a stepwise manner using nitrogen gas. The experimental method for *LOEcrit* determination refers to the method established by Wu et al. [12]. When the fish showed loss of equilibrium, the dissolved oxygen concentration and corresponding time were observed and recorded, and the *LOEcrit* was further calculated using Brett's equation [25].

2.3. Experimental Treatment and Sample Collection

The experiment included a normoxic group, hypoxic stress groups (6, 12, 24 h), and a reoxygenation group (6 h recovery under normoxia). The total number of each experimental fish species is 90. Six fish per species in each group were processed, with the experiment repeated three times. The normoxic group was maintained at a dissolved oxygen (DO) concentration of 7.5 ± 0.1 mg/L. The hypoxic groups had DO stably reduced to 2.0 ± 0.1 mg/L via nitrogen replacement, while the reoxygenation group had dissolved oxygen restored to normoxia by aeration [26].

Before sampling, the experimental fish were anesthetized with 100 mg/L MS-222. After dissection, the second left gill arch was collected and fixed in 1 mL of Bouin's solution for 24 h for subsequent paraffin section preparation. The remaining gill tissue and liver tissue were quickly frozen in liquid nitrogen and then transferred to a −80 °C refrigerator for storage.

2.4. Paraffin Sectioning and Morphological Analysis of Gill Tissue

The fixed gill arches were dehydrated, followed by transparency treatment, paraffin infiltration, embedding, and sectioning. Subsequently, the sections were subjected to dewaxing, rehydration, staining, dehydration, counterstaining, and mounting.

The ImageJ (v. 1.54f, USA) was used to measure the morphological parameters of gill tissue sections, referring to the method proposed by Matey [27]. The measured indicators included the length of gill lamellae extending from the base, the spacing between adjacent gill lamellae, the thickness of gill lamellae, and the thickness of the interlamellar connective tissue matrix (ILCM).

2.5. Determination of Oxidative Stress Indices

The stored liver and gill tissues were ground and centrifuged, and the supernatant was collected and stored on ice for later use. Kits from Nanjing Jiancheng Bioengineering Institute (Nanjing, China) were used to determine the following indicators: catalase (CAT, A007-1-1), superoxide dismutase activity (SOD, A001-3), and malondialdehyde (MDA, A003-1). All indicator determinations were performed strictly in accordance with the kit instructions.

2.6. Gene Cloning and Sequence Analysis

Total RNA was extracted from liver and gill tissues using the Trizol method. Qualified total RNA was used as a template to synthesize the first strand of cDNA with the Prime Script™ RT reagent Kit with gDNA Eraser (Perfect Real Time) (TaKaRa, Kusatsu, Japan). Meanwhile, according to the instructions of the SMART™ RACE cDNA Amplification Kit (Clonetech, Mountain View, CA, USA), 5′-RACE and 3′-RACE templates were synthesized. Based on the CDS sequences of the *hif-1α* and *hif-2α* genes of Blunt snout bream (*hif-1α*: GU363498.1; *hif-2α*: GU363499.1), CDS sequence cloning primers and RACE primers were designed using the Primer Premier 5 software (Table 1). Using cDNA as the template, PCR and 5′/3′-RACE techniques were used for amplification. After identification by agarose gel electrophoresis, the target bands were excised for gel recovery. Positive clones were selected for sequencing through ligation and transformation. Protein domains of Hif-1α and Hif-2α in 2nBY and its parents were analyzed using SMART. Amino acid similarities of Hif-1α and Hif-2α were analyzed with the DNAMAN 6.0 software. Phylogenetic trees were constructed using the Neighbor-Joining (NJ) method in the MEGA 11.0 software.

Table 1. Primer sequences and corresponding applications.

Primer Names	Primer Sequence (5′-3′)	Purpose
hif-1α-F	TGTTGAGAAAGAGAGCCATA	*hif-1α* CDS PCR
hif-1α-R	ATAGATTATTGTGCGACTGT	*hif-1α* CDS PCR
3′-*hif-1α*-1	ACCCCCATGATCCCTGAAAT	*hif-1α* 3′-RACE
3′-*hif-1α*-2	AAGAGCCTTAATGCGAAATA	*hif-1α* 3′-RACE
5′-*hif-1α*-1	TCATTGTAGACGGGCACATCCT	*hif-1α* 5′-RACE
5′-*hif-1α*-2	TTTATGGCTCTCTTTCTCAACA	*hif-1α* 5′-RACE
hif-2α-F	AGAGTTACTGAGTTGATGGGTT	*hif-2α* CDS PCR
hif-2α-R	GTTGTGACTTAGTGGGGGATGA	*hif-2α* CDS PCR
3′-*hif-2α*-1	CTGGACTTGGAGACTCTGGC	*hif-2α* 3′-RACE
3′-*hif-2α*-2	GGTGAGTCATCCCCCACTAA	*hif-2α* 3′-RACE
5′-*hif-2α*-1	AGCCCCCATTCTTAGCCAAC	*hif-2α* 5′-RACE
5′-*hif-2α*-2	CACAGGTTCTGGTGGCTTTT	*hif-2α* 5′-RACE
UPM (Mix)	CTAATACGACTCACTATAGGGCAAGCAGT GGTATCAACGCAGAGT (long)	5′/3′-RACE
	CTAATACGACTCACTATAGGGC (short)	5′/3′-RACE
UPS	CTAATACGACTCACTATAGGGC	5′/3′-RACE

2.7. Quantitative Real-Time PCR Analysis

Quantitative Real-Time PCR primers were designed based on the CDS sequences obtained from gene cloning, with *β-actin* as the reference gene to verify primer specificity (Table 2). The $2^{-\Delta\Delta CT}$ method was used to calculate the relative gene expression levels, and the expression patterns of *hif-1α* and *hif-2α* genes in the liver and gill tissues of different treatment groups were analyzed.

Table 2. qRT-PCR and amplification efficiency.

Primer Names	Primer Sequence (5′-3′)	Amplification Efficiency
q-*hif-1α*-F	AGTCTGTCTGCTCTGGCAACCA	95.5%
q-*hif-1α*-R	TGCGGAGTCTGGAACACGATCA	
q-*hif-2α*-F	CCCACTTCCAGCCCAACATGAG	98.3%
q-*hif-2α*-R	TCGGCAGGATCGTGGTAAGGAG	
q-*β-actin*-F	CGGACAATTTCTCTTTCGGCTG	101.5%
q-*β-actin*-R	ACCCACACCGTGCCCATCTA	

2.8. Data Analysis

All experimental data in this study were processed using Microsoft Excel and expressed as mean ± SD. Statistical analysis was performed with SPSS 19.0. Data normality and homogeneity of variance were tested by Shapiro–Wilk and Levene's tests, respectively. One-way ANOVA and two-way ANOVA were used for intergroup comparisons, followed by Duncan's and LSD post hoc tests. A significance level of $p < 0.05$ was considered statistically significant. Graphs were plotted using GraphPad Prism 9.0, with significant differences marked by different lowercase letters.

3. Results

3.1. Comparison of LOEcrit Among 2nBY and Its Parents

There were significant interspecific differences in the *LOEcrit* of the three fish species. The *LOEcrit* of BSB was the highest, reaching 1.24 mg/L; that of YT was the lowest, at 0.85 mg/L; and the *LOEcrit* of 2nBY was 1.03 mg/L (Figure 1).

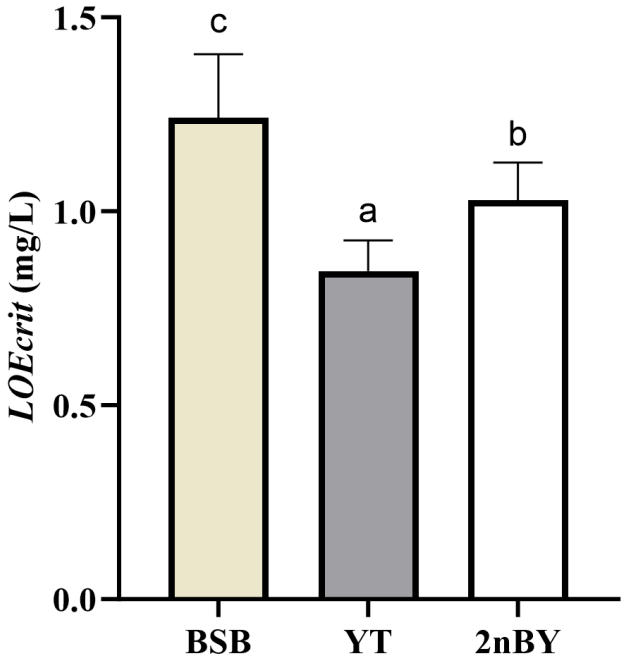


Figure 1. Comparison of *LOEcrit* between 2nBY and its parents. Different letters are significantly different ($p < 0.05$). BSB: blunt snout bream (*Megalobrama amblycephal*), YT: Bleeker's yellow tail (*Xenocypris davidi* Bleeker), 2nBY: the diploid distant hybrid derived from female blunt snout bream (*Megalobrama amblycephal*) × male Bleeker's yellow tail (*Xenocypris davidi* Bleeker). The same below.

3.2. Changes in Gill Tissue Morphology of 2nBY and Its Parents

With the extension of hypoxic stress time, the protruding lamella basal length and the distance between lamellae in the gill tissues of 2nBY and its parents gradually increased. Meanwhile, the protruding lamella thickness and the interlamellar cellular matrix (ILCM) height gradually decreased, and the epithelial cells of gill lamellae gradually separated (Figure 2). After 24 h of hypoxic stress, significant differences were observed in indicators including the protruding lamella basal length, the distance between lamellae, the protruding lamella thickness, and the ILCM height, when compared with the initial state of the normoxic group. Among them, BSB showed the most significant differences (Figure 2). After 6 h of reoxygenation treatment, these morphological characteristics of 2nBY and its parents all recovered to varying degrees, with YT showing the best recovery, followed by 2nBY, and BSB showing the weakest recovery (Figure 3).

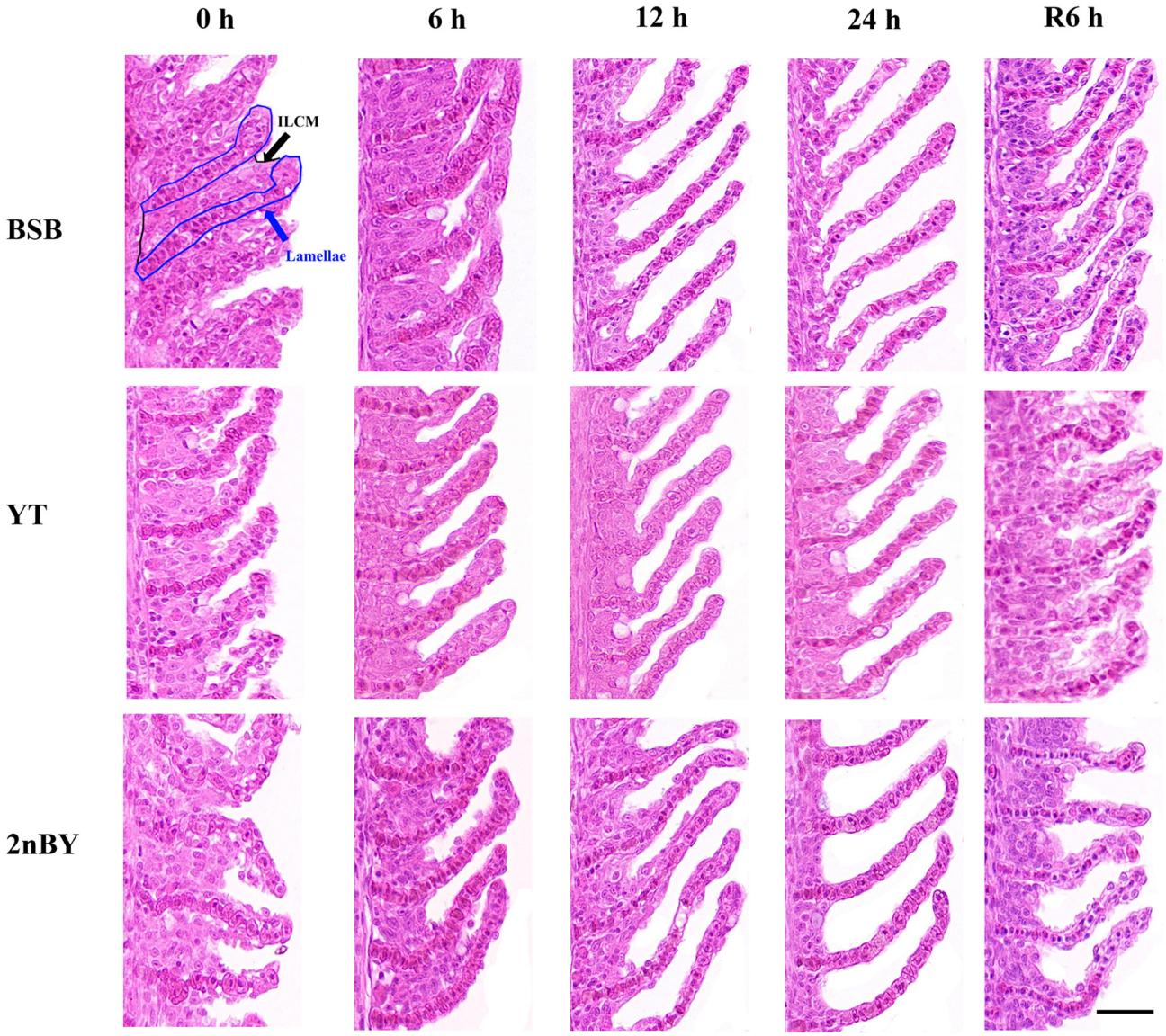


Figure 2. Microstructure of gill tissues of 2nBY and its parents. Additionally, 0, 6, 12 and 24 h indicate the duration of hypoxic stress exposure in the experimental fish, and R6 denotes the duration of reoxygenation. The blue arrows indicate the gill lamellae, and the black arrows indicate the interlamellar cellular matrix (ILCM) groups. Scale bar = 50 μm.

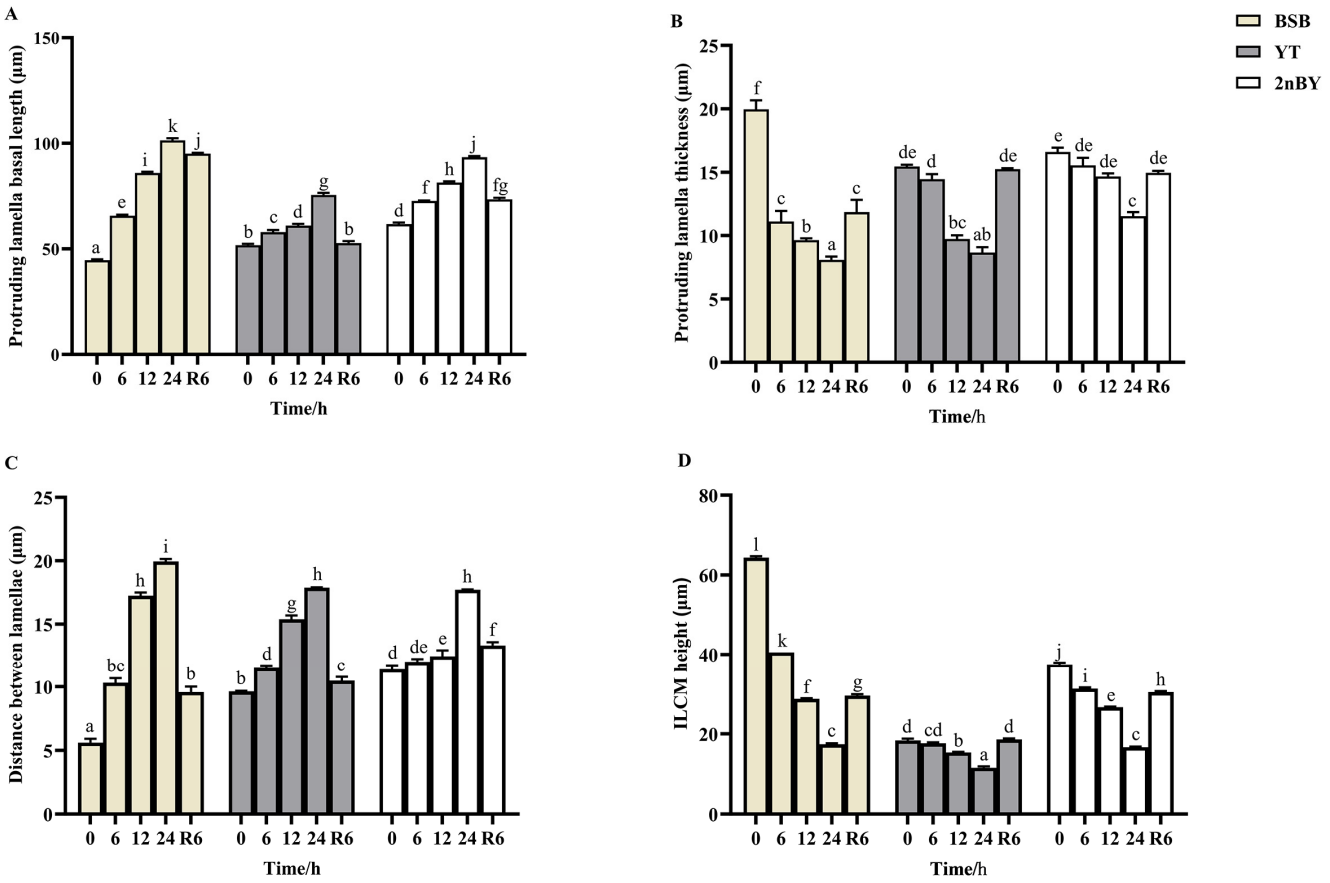


Figure 3. Changes in gill tissue morphological indicators of 2nBY and its parents. (**A**): Protruding lamella basal length; (**B**): protruding lamella thickness; (**C**): distance between lamellae; (**D**): ILCM heights. X-axis labels—0: normoxic group; 6, 12 and 24: hypoxic stress for 6, 12, and 24 h, respectively; R6: reoxygenation for 6 h. Different letters are significantly different ($p < 0.05$).

3.3. Changes in Oxidative Stress Indicators in Gill and Liver Tissues of 2nBY and Its Parents

As the duration of hypoxic stress increased, the SOD and CAT activities and MDA levels of BSB generally showed a gradual upward trend, peaking at 24 h of hypoxic stress. The increases in the activities of SOD and CAT and MDA levels of YT and 2nBY were less significant than those of BSB. After 2nBY and its parents recovered under normoxic conditions for 6h, the SOD and CAT activities and MDA levels decreased significantly approaching the normoxic level, while BSB did not recover to the normoxic level (Figure 4).

3.4. The Full-Length Sequences of hif-1α/2α in 2nBY and Its Parents

The full-length cDNA sequences of the *hif-1α* gene in BSB, YT, and 2nBY were 3850 bp, 3821 bp, and 3859 bp, respectively. The similarity between BSB and 2nBY is 96.7%, and between YT and 2nBY is 98.5%. The corresponding sequences are shown in Supplementary File S1. The full-length cDNA sequences of *hif-2α* in BSB, YT, and 2nBY were 3201 bp, 3203 bp, and 3203 bp, with a similarity of 99.44% between BSB and 2nBY, and 98.69% between YT and 2nBY. The corresponding sequences are shown in Supplementary File S2. The lengths of the 5′-untranslated region (5′-UTR), 3′-untranslated region (3′UTR) and open reading frame (ORF) are shown in Table 3.

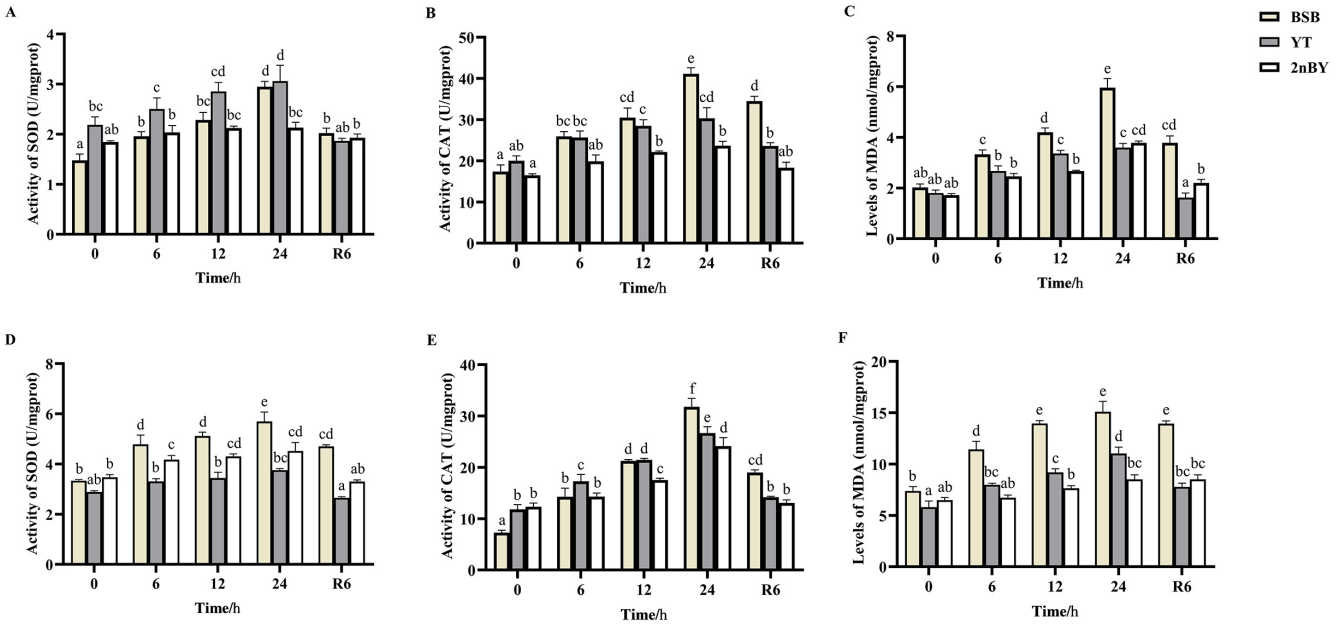


Figure 4. Changes in SOD and CAT activity and MDA levels in liver and gill tissues of 2nBY and its parents under hypoxia and reoxygenation treatments. (**A**–**C**) represent indices determined in the liver, and (**D**–**F**) represent indices determined in the gills. X-axis labels—0: normoxic group; 6, 12 and 24: hypoxic stress for 6, 12, and 24 h, respectively; R6: reoxygenation for 6 h. Different letters are significantly different ($p < 0.05$).

Table 3. Full-length cDNA sequence comparison of *hif-1α/2α* genes in 2nBY and its parents.

	The Full-Length cDNA of *hif-1α*			**The Full-Length cDNA of *hif-2α***		
	5′UTR	ORF	3′UTR	5′UTR	ORF	3′UTR
BSB	283 bp	2325 bp	1242 bp	269 bp	2508 bp	424 bp
YT	248 bp	2322 bp	1251 bp	271 bp	2508 bp	424 bp
2nBY	283 bp	2325 bp	1251 bp	271 bp	2508 bp	424 bp

3.5. Protein Domains and Homology of Hif-1α/2α in 2nBY and Its Parents

SMART conserved domain analysis revealed that both Hif-1α and Hif-2α proteins belong to the bHLH-PAS transcription factor family. The N-termini of the two proteins both contain the bHLH, PAS (including PAS-A and PAS-B), and PAC domains, while the C-termini harbor two transactivation domains, namely N-TAD and C-TAD. The Hif-1α and Hif-2α proteins of 2nBY and its parents exhibit high homology, and all contain the oxygen-dependent degradation domain (ODD) (Figure 5).

3.6. Evolutionary Analysis of Hif-1α/2α in Vertebrates

The phylogenetic tree constructed based on the amino acid sequences of Hif-1α and Hif-2α from multiple species shows that: 2nBY and its parental Hif-1α cluster together as a branch, which then clusters with topmouth gudgeon (*Pseudorasbora parva*) and common carp (*Cyprinus carpio*) to form a larger clade, and further clusters with zebrafish (*Danio rerio*) and mandarin fish (*Siniperca chuatsi*) to form an even larger clade, before finally clustering with the human being (*Homo sapiens*) and chicken (*Gallus gallus*). In contrast, the evolutionary branching pattern of Hif-2α differs from that of Hif-1α: 2nBY and its parental Hif-2α first cluster with zebrafish and mandarin fish to form a branch, then cluster with topmouth gudgeon and common carp to form a larger clade, and finally cluster with the human being and chicken (Figure 6).

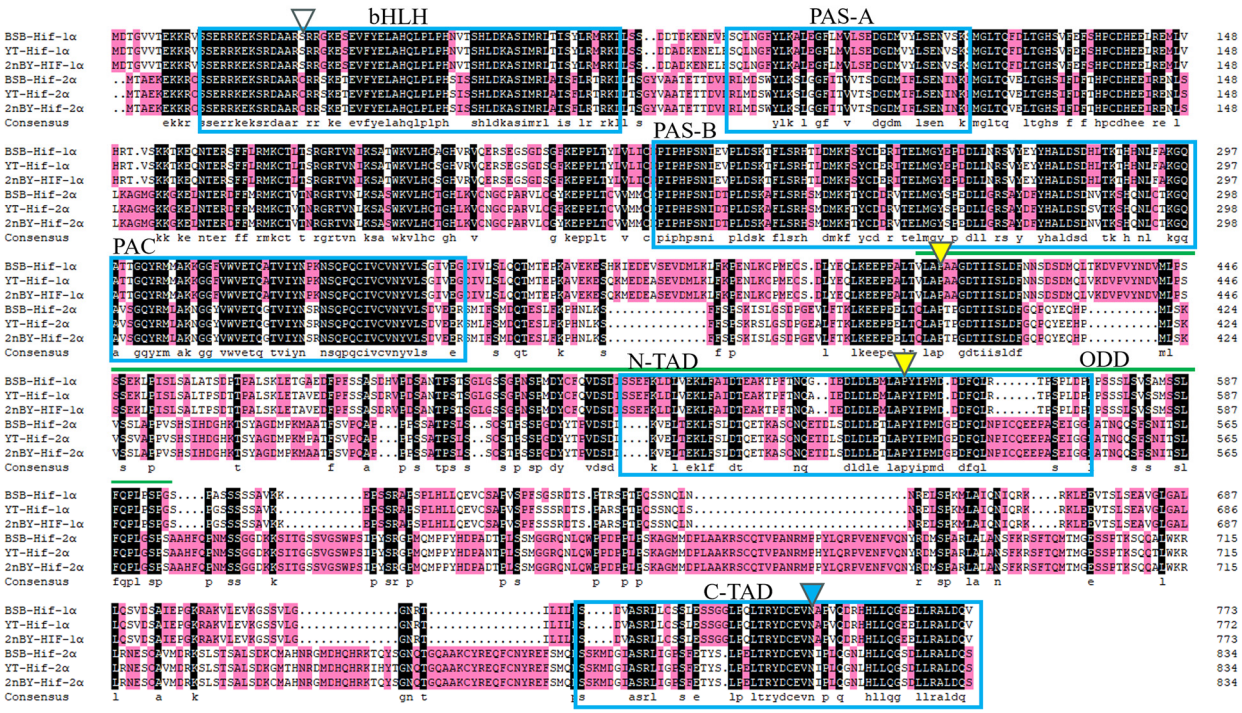


Figure 5. Conserved domains of Hif-1α and Hif-2α of 2nBY and its parents. Pink letters indicate amino acid similarity > 50%, black letters indicate amino acid similarity = 100%. Blue boxes indicate conserved protein domains; yellow inverted triangles mark 2 conserved proline residues in the ODD; green straight lines indicate the ODD; white inverted triangles mark serine in the bHLH domain; blue inverted triangles mark aspartic acid residues in the C-TAD domain; lowercase letters: identical amino acids.

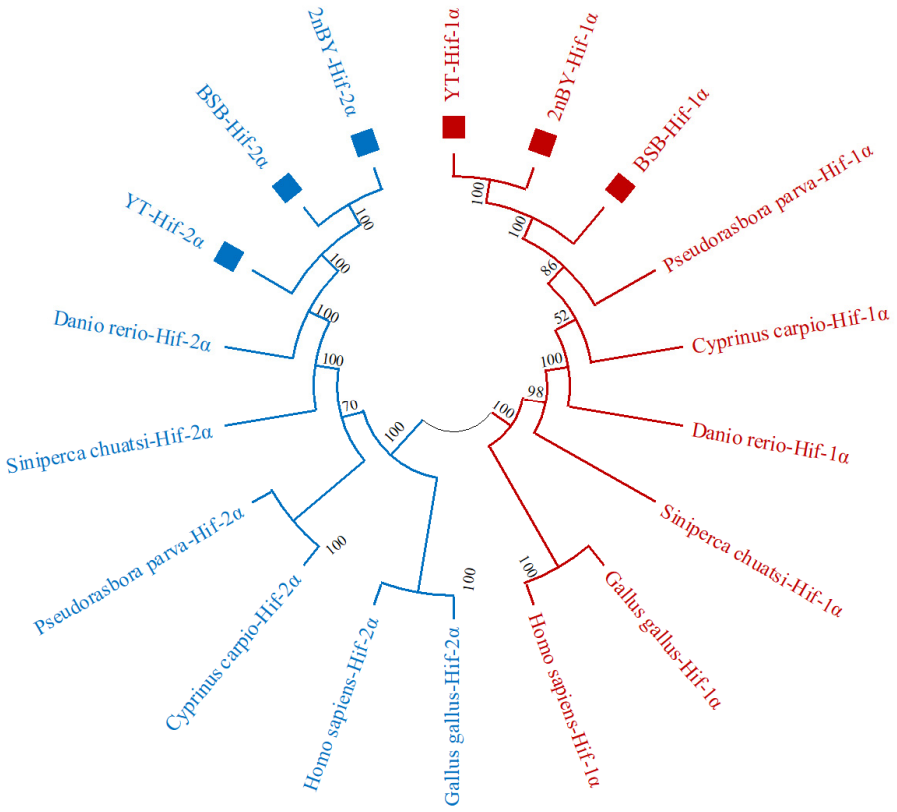


Figure 6. Phylogenetic trees of Hif-1α and Hif-2α in vertebrates. The red part indicates the evolutionary path of Hif-1α, and the blue part indicates the evolutionary path of Hif-2α. Values on the branches represent

bootstrap support (%). The sequences used for comparison and their GenBank accession numbers were as following: *Cyprinus carpio* (Hif-1α: ADW54531.1; Hif-2α: XP_042591456.1), *Danio rerio* (Hif-1α: NP_001296971.1; Hif-2α: ABD33838.1), *Homo sapiens* (Hif-1α: WPD49272.1; Hif-2α: NP_001421.2), *Gallus gallus* (Hif-1α: NP_989628.2; Hif-2α: NP_990138.2), *Pseudorasbora parva* (Hif-1α: ACO35259.1; Hif-2α: XP_067286485.1), *Siniperca chuatsi* (Hif-1α: QDA76729.1; Hif-2α: XP_044070053.1). Amino acid sequences of full-length HIF-αs were analyzed using the neighbor-joining method in the MEGA 11 program. Gaps were removed from the alignment. The bootstrap values derived from 1000 replications are shown.

3.7. Expression Patterns of *hif-1α/hif-2α* in Liver and Gill Tissues of 2nBY and Its Parents

In the liver tissue: After 24 h of hypoxic stress, the expressions of *hif-1α* and *hif-2α* in the three fish species (BSB, 2nBY, YT) were all significantly upregulated. Among them, BSB showed the largest upregulation amplitude, followed by 2nBY and YT. After reoxygenation, the expressions of the two genes in 2nBY and YT returned to the normoxic level, while those in BSB remained significantly higher than the normoxic group (Figure 7A,B). In the gill tissue: After 24 h of hypoxic stress, the expression of *hif-1α* in BSB was significantly downregulated, while that in 2nBY and YT was significantly upregulated; meanwhile, the expressions of *hif-2α* in BSB and 2nBY were both significantly upregulated. After 6 h of reoxygenation, the expression of *hif-2α* in 2nBY returned to the normoxic level, that in BSB did not recover, and there was no significant difference in the expression of *hif-2α* in the gill tissue of YT compared with the normoxic group (Figure 7C,D).

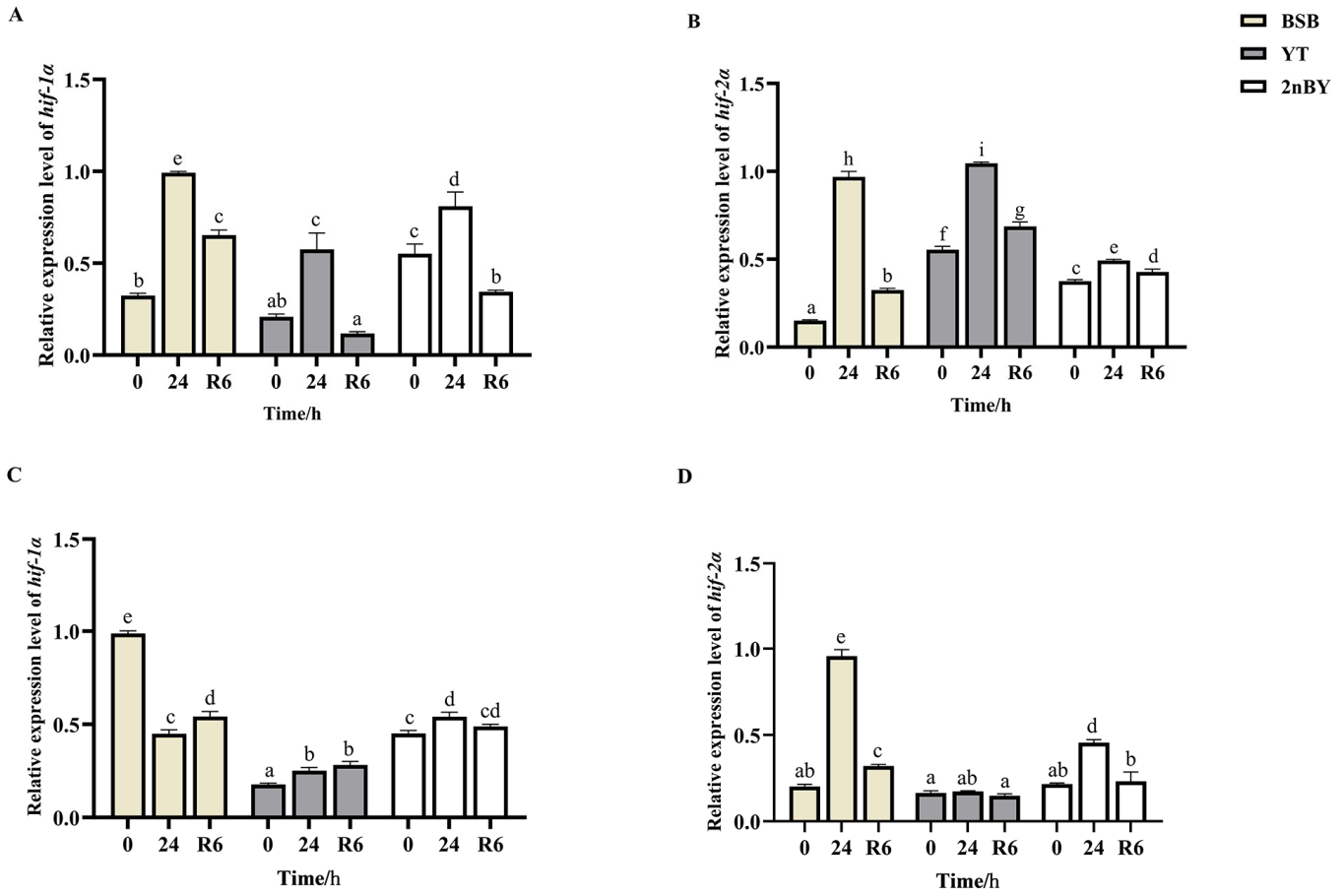


Figure 7. Changes in the expression of *hif-1α/2α* in liver and gill tissues of 2nBY and its parents under hypoxia and reoxygenation treatments. (**A**,**B**) Expression changes in *hif-1α/2α* genes in liver tissue; (**C**,**D**) expression changes in *hif-1α/2α* genes in gill tissue; 0: normoxic group; 24: hypoxic stress for 24 h; R6: reoxygenation for 6 h. Different letters are significantly different ($p < 0.05$).

4. Discussion

Aquaculture is a crucial industry for ensuring high quality protein supply. However, hypoxia stress caused by fluctuations in the dissolved oxygen (DO) levels in water has been demonstrated to be a key environmental factor restricting fish growth and survival, threatening aquaculture efficiency [28]. *LOEcrit* is a core behavioral indicator for evaluating the hypoxia tolerance of fish, with lower values indicating stronger hypoxia tolerance [29]. In this study, the *LOEcrit* of 2nBY was significantly lower than that of BSB and fell between the two parental species. The results indicate that compared with BSB, 2nBY has a substantially improved hypoxia tolerance. It is worth noting that there is a difference between the *LOEcrit* result of BSB obtained in this experiment and that determined by Wu Chengbin [12], which may be related to differences in the body mass of the experimental fish, as well as the temperature, salinity and pH of the test water [30].

In previous studies, significant structural changes have been found to occur in the gills of fish subjected to hypoxia and reoxygenation, such as grass carp (*Ctenopharyngodon Idella*) and Pangasius sutchi (*Pangasianodon hypophthalmus*) [31,32]. Similarly, this study found that the protrusion length of gill lamellae from the base and the spacing between adjacent gill lamellae in 2nBY and its parents gradually increased, while the interlamellar matrix and thickness of gill lamellae gradually decreased, with partial recovery after reoxygenation. This indicates that 2nBY and its parents possess gill remodeling ability. Differences in gill remodeling ability among the three groups were observed from the changes in gill tissue structure after 6 h of reoxygenation: YT showed the fastest recovery, 2nBY was between the two parents, and BSB was the slowest. Compared with BSB, the hybrid fish also exhibited a faster recovery rate [33]. Both 2nBY and YT have a stronger gill remodeling capacity than BSB, which may be one of the reasons for their superior hypoxia tolerance.

Changes in the activity of SOD and CAT and levels of MDA can directly reflect the degree of oxidative damage to the organism and the regulatory capacity of its antioxidant system [34]. In this study, after 24 h of hypoxia, the increase in the SOD and CAT activity in the liver and gill tissues of BSB was significantly higher than that in 2nBY and YT. Moreover, the SOD and CAT activity in BSB did not return to the normoxic level even after 6 h of reoxygenation. This result is consistent with the trend of levels changes in "Pujiang No.2" and crucian carp [11,34]. In addition, as a marker of oxidative damage, the levels of MDA in the liver and gill tissues of BSB increased significantly with the extension of hypoxia time, and this trend was consistent with that of mandarin fish and yellow catfish (*Pelteobagrus fulvidraco*) [18,35]. The change in MDA levels in YT and 2nBY was less significant than that in BSB. After 6 h of reoxygenation, the levels of oxidative stress markers in the two species basically returned to the normoxic level, while those in BSB were still significantly higher than the normoxic group. It is speculated that the antioxidant system of BSB was damaged due to the destruction of a large number of reactive free radicals, so it could not return to the normoxic level in a short time. Furthermore, the recovery rate of the F_3 generation of *Megalobrama amblycephala* × *Culter alburnus* was also faster than that of its female parent BSB [33].

Given the crucial roles of Hif-1α and Hif-2α in the hypoxic regulation of fish, this study obtained the full-length cDNAs of the *hif-1α* and *hif-2α* genes from 2nBY and its parents. Sequence alignment of *hif-1α* among the three showed 96.70% similarity between BSB and 2nBY, and 98.50% similarity between YT and 2nBY. For *hif-2α*, the similarity between BSB and 2nBY was 99.44%, while that between YT and 2nBY was 98.69%. 2nBY and its parents exhibit high homology. Prediction of the conserved domains of the two proteins revealed that both Hif-1α and Hif-2α contain six conserved protein domains: bHLH, PAS-A, PAS-B, PAC, N-TAD, and C-TAD. Among these domains, bHLH, PAS (including PAS-A/PAS-B), and PAC are located at the N-terminus. They can form a heterodimer

with Hif-β, bind to the hypoxia-responsive element (HRE) of DNA, and then interact with other transcriptional activators to regulate physiological functions [36]. Unlike Hif-1α, Hif-2α contains a cysteine residue in the bHLH domain, which makes it more oxygen-sensitive and prone to DNA binding. This feature may enable Hif-2α to play a more important role in hypoxic regulation [37]. The two transcriptional activation domains, N-TAD and C-TAD, are located at the C-terminus. They can bind to the coactivators p300/CBP and achieve precise regulation of gene transcriptional activation through the hydroxylation of conserved aspartic acid residues [38,39]. In addition, both proteins contain an oxygen-dependent degradation domain (ODD). Under normoxic conditions, specific proline residues in the ODD undergo hydroxylation (Pro402 and Pro564 in Hif-1α; Pro405 and Pro531 in Hif-2α). This process destabilizes the Hif-α subunit, leading to its rapid degradation. This mechanism regulates the intracellular level of Hif-α, ensuring that Hif-αs accumulate only under hypoxic conditions and maintaining the cell's sensitivity and responsiveness to oxygen [40,41]. The ODD of Hif-1α/2α from 2nBY and its parental species contain conserved proline residues, which are involved in oxygen-dependent degradation regulation [38]. In the phylogenetic trees of Hif-1α and Hif-2α, Hif-1α shows high conservation among Cyprinidae fish, while Hif-2α is not as genetically stable as Hif-1α in Cyprinidae fish and evolves faster than Hif-1α.

Hypoxia often threatens fish survival and development, so different fish species have evolved unique molecular mechanisms to counter hypoxic damage [42]. This study analyzed the expression of *hif-1α/2α* in the liver and gill tissues of 2nBY and its parental species under hypoxia and reoxygenation. This is similar to the mechanism by which naked carp (*Gymnocypris dobula*) in the Tibet region adapts to long-term hypoxia by downregulating *hif-1α* and *hif-2α* [43]. After 24h of hypoxia, *hif-1α/2α* was significantly upregulated in the liver of all three groups [44],with BSB showing the largest upregulation. This suggests Hif-1α and Hif-2α of 2nBY have higher stability under hypoxia, enabling effective activation of downstream signaling pathways without substantial transcriptional elevation. In gill tissue, the expression of *hif-1α* in BSB was significantly downregulated, which is consistent with the results in silver carp (*Hypophthalmichthys molitrix*) [2], while *hif-1α* was upregulated in 2nBY and YT, in line with the findings in grass carp [21]. The differential expression of *hif-1α* may be one of the reasons why BSB is difficult to adapt to hypoxia. The expression of *hif-2α* was significantly upregulated in 2nBY and BSB, but no significant change was observed in YT. After 6 h of reoxygenation, the expression of *hif-1α/2α* in the liver and gill tissues of YT and 2nBY quickly recovered to normoxic levels, whereas BSB showed slower and incomplete recovery. It can be inferred that YT and 2nBY have a stronger feedback regulation ability of the oxygen-sensing system to prevent tissue oxidative damage.

During long term evolution, fish have developed a series of adaptive strategies to cope with hypoxic environments. These strategies involve multiple aspects such as respiratory regulation [30], energy metabolism [5], oxidative stress defense [11], and immune regulation [45]. Regulatory processes at different levels are interconnected and jointly maintain the physiological homeostasis of the organism under hypoxic conditions. The multi-level mechanisms of hypoxia adaptation in 2nBY still need to be further explored.

5. Conclusions

After hypoxic and reoxygenation treatment, a comparison of *LOEcrit*, changes in gill tissue structure and antioxidant indices, as well as differences in the expression regulation of *hif-1α/2α* between 2nBY and its parents, revealed that 2nBY has better hypoxia tolerance and stronger recovery ability than BSB, and these advantages may be derived from YT. These results provide theoretical and technical support for the breeding of a new hypoxia-tolerant germplasm resource of bream.

Supplementary Materials: The following supporting information can be downloaded at: https://www.mdpi.com/article/10.3390/fishes11040233/s1, File S1: The full-length cDNA sequences of the *hif-1α* gene in BSB, YT, and 2nBY; File S2: The full-length cDNA sequences of *hif-2α* in BSB, YT, and 2nBY.

Author Contributions: Conceptualization, Z.T. and S.F.; methodology, Z.T., S.F. and X.Y.; validation, Z.T. and X.Y.; formal analysis, C.Z. and J.L.; investigation, Z.T., X.Y. and X.C.; resources, Z.Z. and F.Y.; data curation, Z.T. and J.L.; writing—original draft preparation, Z.T.; writing—review and editing, M.T., S.F. and Z.T.; visualization, Z.T. and Y.T.; supervision, M.T. and C.Z.; project administration, M.T.; funding acquisition, M.T. All authors have read and agreed to the published version of the manuscript.

Funding: This research was supported by the National Key Research and Development Plan Program of China (Grant No. 2022YFD2400600/2022YFD2400601), the Yuelushan Laboratory Breeding Program (Grant No. YLS-2025-ZY01011), the National Natural Science Foundation of China (Grant No. 32293252, 32293253), the Hunan Province Science and Technology Innovation Platform and Talent Program leading talent (Grant No. 2023RC1053), and the Earmarked Fund for China Agriculture Research System (CARS-45).

Institutional Review Board Statement: The animal protocol utilized in this study was approved by the Ethics Committee of Hunan Normal University (Approval Code 610; Approval Date: 23 July 2025). All procedures strictly complied with the Administration of Affairs Concerning Animal Experimentation Guidelines (China) and institutional animal welfare policies.

Data Availability Statement: Data will be made available on request. The original contributions presented in this study are included in the article. Further inquiries can be directed to the corresponding authors.

Conflicts of Interest: The authors declare no conflicts of interest.

References

1. Chen, S.Y.; Wang, F.; Song, J.L.; Li, F.; Wang, J.W.; Jia, Y.D. Sexual dimorphism in physiological responses of turbot (*Scophthalmus maximus* L) under acute hypoxia and reoxygenation. *Aquaculture* **2025**, *595*, 741614. [CrossRef]
2. Li, X.H.; Ling, C.; Wang, Q.X.; Feng, C.; Luo, X.Z.; Sha, H.; He, G.Y.; Zou, G.W.; Liang, H.W. Hypoxia stress induces tissue damage, immune defense, and oxygen transport change in gill of silver carp (*Hypophthalmichthys molitrix*): Evaluation on hypoxia by using transcriptomics. *Front. Mar. Sci.* **2022**, *9*, 900200. [CrossRef]
3. Sun, H.; Li, J.; Tang, L.; Yang, Z. Responses of crucian carp *Carassius auratus* to long-term exposure to nitrite and low dissolved oxygen levels. *Biochem. Syst. Ecol.* **2012**, *44*, 224–232. [CrossRef]
4. Zhang, Z.W.; Li, Z.; Liang, H.W.; Li, L.; Luo, X.H.; Zou, G.W. Molecular cloning and differential expression patterns of copper/zinc superoxide dismutase and manganese superoxide dismutase in *Hypophthalmichthys molitrix*. *Fish Shellfish Immunol.* **2011**, *30*, 473–479. [CrossRef]
5. Mandic, M.; Todgham, A.E.; Richards, J.G. Mechanisms and evolution of hypoxia tolerance in fish. *Proc. R. Soc. B Biol. Sci.* **2009**, *276*, 735–744. [CrossRef]
6. Wang, S.; Tang, C.C.; Tao, M.; Qin, Q.B.; Zhang, C.; Luo, K.K.; Zhao, R.R.; Wang, J.; Ren, L.; Xiao, J.J.S.C.L.S. Establishment and application of distant hybridization technology in fish. *Sci. China Life Sci.* **2019**, *62*, 22–45. [CrossRef]
7. Chen, N.; Wu, M.; Tang, G.P.; Wang, H.J.; Huang, C.X.; Wu, X.J.; He, Y.; Zhang, B.; Huang, C.H.; Liu, H. Effects of acute hypoxia and reoxygenation on physiological and immune responses and redox balance of Wuchang bream (*Megalobrama amblycephala* Yih, 1955). *Front. Physiol.* **2017**, *8*, 375. [CrossRef]
8. Tang, Y.T.; Wang, C.; Jiang, H.J.; Zhao, L.J.; Qian, C.; Guo, X.S.; Sun, Y.F.; Tang, B.P.; Xuan, F.J.; Cheng, Y.X. Grazing effects of *Xenocypris davidi* Bleeker (*Cyprinidae, Cypriniformes*) on filamentous algae and the consequent effects on intestinal microbiota. *Aquac. Res.* **2023**, *2023*, 1985865. [CrossRef]
9. Hu, J.; Liu, S.J.; Xiao, J.; Zhou, Y.; You, C.P.; He, W.G.; Zhao, R.R.; Song, C.; Liu, Y. Characteristics of diploid and triploid hybrids derived from female *Megalobrama amblycephala* Yih× male *Xenocypris davidi* Bleeker. *Aquaculture* **2012**, *364*, 157–164. [CrossRef]
10. Fan, S.Y.; Tang, Z.; Wang, Y.Q.; Zhou, Z.F.; Wu, C.; Luo, K.K.; Hu, J.; Gong, D.B.; Li, S.N.; Tao, M. The bisexual natural gynogenetic blunt snout bream lineage derived from the distant hybridization of female blunt snout bream and male Bleeker's yellow tail. *Aquac. Rep.* **2024**, *37*, 102206. [CrossRef]
11. Yu, X.X.; Zhang, Y.R.; Li, S.S.; Zheng, G.D.; Zou, S.M. Effects of hypoxia on the gill morphological structure, apoptosis and hypoxia-related gene expression in blunt snout bream (*Megalobrama amblycephala*). *Fish Physiol. Biochem.* **2023**, *49*, 939–949. [CrossRef] [PubMed]

12. Wu, C.B.; Liu, Z.Y.; Li, F.G.; Chen, J.; Jiang, X.Y.; Zou, S.M. Gill remodeling in response to hypoxia and temperature occurs in the hypoxia sensitive blunt snout bream (*Megalobrama amblycephala*). *Aquaculture* **2017**, *479*, 479–486. [CrossRef]
13. Márián, T.; Krasznai, Z.; Balkay, L.; Balazs, M.; Emri, M.; Bene, L.; Tron, L. Hypo-osmotic shock induces an osmolality-dependent permeabilization and structural changes in the membrane of carp sperm. *J. Histochem. Cytochem.* **1993**, *41*, 291–297. [CrossRef]
14. Sollid, J.; Nilsson, G.E. Plasticity of respiratory structures—Adaptive remodeling of fish gills induced by ambient oxygen and temperature. *Respir. Physiol. Neurobiol.* **2006**, *154*, 241–251. [CrossRef]
15. Rojas, I.; De Mello, M.M.; Zanuzzo, F.S.; Sandrelli, R.M.; C Peroni, E.F.; Hall, J.R.; Rise, M.L.; Urbinati, E.C.; Gamperl, A.K. Chronic Hypoxia Has Differential Effects on Constitutive and Antigen-Stimulated Immune Function in Atlantic Salmon (*Salmo salar*). *Front. Immunol.* **2025**, *16*, 1545754. [CrossRef]
16. Li, Y.; Li, T.; Yao, M.; Li, C.; Jiang, Z.; Pan, H.; Wang, W.; Li, Y.; Zhou, H. Metabolic Responses and Oxidative Stress Adaptation Mechanisms of the Pituitary Gland in the Tiger Puffer Under Low-Temperature Stress. *Fishes* **2025**, *10*, 572. [CrossRef]
17. Zhang, G.; Mao, J.; Liang, F.; Chen, J.; Zhao, C.; Yin, S.; Wang, L.; Tang, Z.; Chen, S. Modulated expression and enzymatic activities of Darkbarbel catfish, *Pelteobagrus vachelli* for oxidative stress induced by acute hypoxia and reoxygenation. *Chemosphere* **2016**, *151*, 271–279. [CrossRef]
18. Ding, W.D.; Cao, L.P.; Cao, Z.M.; Bing, X.W. Transcriptomic responses of the liver of mandarin fish (*Siniperca chuatsi*) under hypoxic stress. *J. Fish Biol.* **2023**, *103*, 44–58. [CrossRef]
19. Krzywinska, E.; Stockmann, C. Hypoxia, metabolism and immune cell function. *Biomedicines* **2018**, *6*, 56. [CrossRef]
20. Sun, X.; Zhu, C.; Liu, W.; Wang, Z.; Deng, H.; Jia, S.; Bai, Y.; Xiao, W.; Liu, X. Loss of one copy of v*hl* in zebrafish facilitates hypoxia tolerance. *Aquac. Rep.* **2023**, *33*, 101782. [CrossRef]
21. Law, S.H.; Wu, R.S.; Ng, P.K.; Yu, R.M.; Kong, R.Y. Cloning and expression analysis of two distinct HIF-alpha isoforms–gcHIF-1alpha and gcHIF-4alpha–from the hypoxia-tolerant grass carp, *Ctenopharyngodon idellus*. *BMC Mol. Biol.* **2006**, *7*, 15. [CrossRef]
22. Ravenna, L.; Salvatori, L.; Russo, M.A. HIF 3α: The little we know. *FEBS J.* **2016**, *283*, 993–1003. [CrossRef] [PubMed]
23. Hoefflin, R.; Harlander, S.; Schäfer, S.; Metzger, P.; Kuo, F.; Schönenberger, D.; Adlesic, M.; Peighambari, A.; Seidel, P.; Chen, C.-y. HIF-1α and HIF-2α differently regulate tumour development and inflammation of clear cell renal cell carcinoma in mice. *Nat. Commun.* **2020**, *11*, 4111. [CrossRef] [PubMed]
24. Peng, Z.; Liu, X.; Jin, M.; Zhan, Y.; Zhang, X.; Bao, Y.; Liu, M. Hypoxia Activates *HIF-1α* and Affects Gene Expression and Transcriptional Regulation of *PHD* in *Tegillarca granosa*. *Fishes* **2023**, *8*, 359. [CrossRef]
25. Brett, J.R. The respiratory metabolism and swimming performance of young sockeye salmon. *J. Fish. Board Can.* **1964**, *21*, 1183–1226. [CrossRef]
26. Shuang, L.; Su, X.L.; Zheng, G.D.; Zou, S.M. Effects of hypoxia and reoxygenation on gill remodeling, apoptosis, and oxidative stress in hypoxia-tolerant new variety blunt snout bream *(Megalobrama amblycephala*). *Fish Physiol. Biochem.* **2022**, *48*, 263–274. [CrossRef]
27. Matey, V.; Richards, J.G.; Wang, Y.X.; Wood, C.M.; Rogers, J.; Davies, R.; Murray, B.W.; Chen, X.Q.; Du, J.; Brauner, C.J. The effect of hypoxia on gill morphology and ionoregulatory status in the Lake Qinghai scaleless carp, *Gymnocypris przewalskii*. *J. Exp. Biol.* **2008**, *211*, 1063–1074. [CrossRef]
28. Kulkarni, S.J. A review on research and studies on dissolved oxygen and its affecting parameters. *Int. J. Res. Rev.* **2016**, *3*, 18–22.
29. Wen, M.; Zhu, C.C.; Tang, Y.H.; Zhang, H.; Liu, Z.; Wang, S.Y.; Tao, M.; Hu, L.; Rao, W.T.; Li, S.N. Mechanism of hypoxia tolerance improvement in hybrid fish Hefang bream. *Aquaculture* **2025**, *599*, 742199. [CrossRef]
30. Kramer, D.L. Dissolved oxygen and fish behavior. *Environ. Biol. Fishes* **1987**, *18*, 81–92. [CrossRef]
31. Xu, X.N.; Chen, S.L.; Jiang, Z.X.; un Nissa, M.; Zou, S.M. Gill remodeling increases the respiratory surface area of grass carp (*Ctenopharyngodon idella*) under hypoxic stress. *Comp. Biochem. Physiol. Part A Mol. Integr. Physiol.* **2022**, *272*, 111278. [CrossRef] [PubMed]
32. Phuong, L.M.; Nyengaard, J.R.; Bayley, M. Gill remodelling and growth rate of striped catfish *Pangasianodon hypophthalmus* under impacts of hypoxia and temperature. *Comp. Biochem. Physiol. Part A Mol. Integr. Physiol.* **2017**, *203*, 288–296. [CrossRef] [PubMed]
33. Chen, S.L.; Xu, W.Y.; Shuang, L.; Wen, J.; Zheng, G.D.; Zou, S.M. Evaluation of hypoxia tolerance in F_3 hybrids of blunt snout bream (*Megalobrama amblycephala*♀) × topmouth culter (*Culter alburnus*♂). *Aquaculture* **2023**, *573*, 739589. [CrossRef]
34. Zhao, Y.; Jiang, X.; Kong, X.; Di, G.; Nie, G.; Li, X. Effects of hypoxia on lysozyme activity and antioxidant defences in the kidney and spleen of *Carassius auratus*. *Aquac. Res.* **2017**, *48*, 223–235. [CrossRef]
35. Wang, J.; Li, L.; Zhao, S.S.; Wang, M.; Li, B.; Guo, H.X.; Han, D.; Zhu, X.M.; Zhang, L. Combined effects of prolonged temperature and hypoxia stress on growth, metabolism and physiological status of yellow catfish (*Pelteobagrus fulvidraco*). *Aquac. Rep.* **2025**, *43*, 102884. [CrossRef]
36. Bruick, R.K. Oxygen sensing in the hypoxic response pathway: Regulation of the hypoxia-inducible transcription factor. *Genes Dev.* **2003**, *17*, 2614–2623. [CrossRef]
37. Lando, D.; Pongratz, I.; Poellinger, L.; Whitelaw, M.L. A redox mechanism controls differential DNA binding activities of hypoxia-inducible factor (HIF) 1α and the HIF-like factor. *J. Biol. Chem.* **2000**, *275*, 4618–4627. [CrossRef]

38. Lando, D.; Peet, D.J.; Whelan, D.A.; Gorman, J.J.; Whitelaw, M.L. Asparagine hydroxylation of the HIF transactivation domain: A hypoxic switch. *Science* **2002**, *295*, 858–861. [CrossRef]
39. Cao, Y.; Chen, X.Q.; Wang, S.; Wang, Y.X.; Du, J.Z. Evolution and regulation of the downstream gene of hypoxia-inducible factor-1α in naked carp (*Gymnocypris przewalskii*) from Lake Qinghai, China. *J. Mol. Evol.* **2008**, *67*, 570–580. [CrossRef]
40. Percy, M.J.; Mooney, S.M.; McMullin, M.F.; Flores, A.; Lappin, T.R.; Lee, F.S. A common polymorphism in the oxygen-dependent degradation (ODD) domain of hypoxia inducible factor-1α (HIF-1α) does not impair Pro-564 hydroxylation. *Mol. Cancer* **2003**, *2*, 31. [CrossRef]
41. Figg, W.D., Jr.; Fiorini, G.; Chowdhury, R.; Nakashima, Y.; Tumber, A.; McDonough, M.A.; Schofield, C.J. Structural basis for binding of the renal carcinoma target hypoxia-inducible factor 2α to prolyl hydroxylase domain 2. *Proteins Struct. Funct. Bioinform.* **2023**, *91*, 1510–1524. [CrossRef]
42. Zhong, X.P.; Wang, D.; Zhang, Y.B.; Gui, J.F. Identification and characterization of hypoxia-induced genes in *Carassius auratus* blastulae embryonic cells using suppression subtractive hybridization. *Comp. Biochem. Physiol. Part B Biochem. Mol. Biol.* **2009**, *152*, 161–170. [CrossRef]
43. Guan, L.; Chi, W.; Xiao, W.H.; Chen, L.B.; He, S.P. Analysis of hypoxia-inducible factor alpha polyploidization reveals adaptation to Tibetan plateau in the evolution of schizothoracine fish. *BMC Evol. Biol.* **2014**, *14*, 192. [CrossRef]
44. Terova, G.; Rimoldi, S.; Corà, S.; Bernardini, G.; Gornati, R.; Saroglia, M. Acute and chronic hypoxia affects HIF-1α mRNA levels in sea bass (*Dicentrarchus labrax*). *Aquaculture* **2008**, *279*, 150–159. [CrossRef]
45. Douxfils, J.; Deprez, M.; Mandiki, S.; Milla, S.; Henrotte, E.; Mathieu, C.; Silvestre, F.; Vandecan, M.; Rougeot, C.; Mélard, C. Physiological and proteomic responses to single and repeated hypoxia in juvenile Eurasian perch under domestication–clues to physiological acclimation and humoral immune modulations. *Fish Shellfish Immunol.* **2012**, *33*, 1112–1122. [CrossRef]

Disclaimer/Publisher's Note: The statements, opinions and data contained in all publications are solely those of the individual author(s) and contributor(s) and not of MDPI and/or the editor(s). MDPI and/or the editor(s) disclaim responsibility for any injury to people or property resulting from any ideas, methods, instructions or products referred to in the content.